



# Aggressive Environment Resistance of Concrete Products Modified With Nano Alumina and Nano Silica

Yao Zhao<sup>1</sup>, Na Cui<sup>1\*</sup>, Shuyuan Zhao<sup>2\*</sup>, Yunzhe Zhu<sup>2</sup>, Pengkun Hou<sup>1</sup>, Lichao Feng<sup>3</sup> and Ning Xie<sup>1,2\*</sup>

<sup>1</sup>Shandong Provincial Key Laboratory of Preparation and Measurement of Building Materials and School of Civil Engineering and Architecture, University of Jinan, Jinan, China, <sup>2</sup>Center for Composite Materials, Harbin Institute of Technology, Harbin, China, <sup>3</sup>Jiangsu Marine Resources Development Research Institute and School of Mechanical Engineering, Jiangsu Ocean University, Lianyungang, China

## OPEN ACCESS

### Edited by:

Maria Konsta-Gdoutos,  
University of Texas at Arlington,  
United States

### Reviewed by:

Ali Behnood,  
Purdue University, United States  
Pan Wang,  
Qingdao University of Technology,  
China

### \*Correspondence:

Na Cui  
cea\_cuin@ujn.edu.cn  
Shuyuan Zhao  
angel.zsy@hit.edu.cn  
Ning Xie  
xieningmt@163.com

### Specialty section:

This article was submitted to  
Structural Materials,  
a section of the journal  
Frontiers in Materials

Received: 15 April 2021

Accepted: 04 June 2021

Published: 18 June 2021

### Citation:

Zhao Y, Cui N, Zhao S, Zhu Y, Hou P,  
Feng L and Xie N (2021) Aggressive  
Environment Resistance of Concrete  
Products Modified With Nano Alumina  
and Nano Silica.  
Front. Mater. 8:695624.  
doi: 10.3389/fmats.2021.695624

The service life of concrete products with exposure to an aggressive environment has raised great concerns in the past decades. Nanomaterials have been used as a promising approach to improve the environmental resistance of concrete products when exposed to synergistic attacks. The impacts of  $\text{CaCl}_2$  on nano-modified concrete, especially along with freeze/thaw (F/T) and wet/dry (W/D) cycles, were barely discussed. In this study, the impacts of  $\text{CaCl}_2$  along with F/T and W/D cycles on the nano  $\text{SiO}_2$  and  $\text{Al}_2\text{O}_3$  modified concrete were investigated. The mass loss, flexural strength, compressive strength, and relative dynamic modulus of elasticity were tested to evaluate the durability of concrete products. The testing results indicate that the addition of nanoparticles has a distinctive effect on the environment resistance enhancement of concrete samples. The microstructure analysis demonstrates that with the addition of nanoparticles, high-density hydration products were formed, which is beneficial to the properties enhancement of concrete products. This study not only provides an approach to realize the nano modification on the durability of concrete products but also helps to design and fabricate environmentally resistant concrete products when exposed to a synergistic aggressive environment.

**Keywords:** chemical resistance, concrete products, nano modification, microstructure analysis, deleterious mechanism

## INTRODUCTION

In cold regions, chemicals have been widely utilized as deicers to control the ice and snow on the road. Despite using deicing chemicals can significantly improve transportation efficiency and mitigate the damage from traffic accidents in the winter season, the side effect of using deicing chemicals is also inevitable. Currently, the widely used deicing chemicals include  $\text{NaCl}$ ,  $\text{MgCl}_2$ ,  $\text{CaCl}_2$ , and even  $\text{CaAc}_2$ . It has been widely accepted that the concrete products will severely deteriorate when exposed to aggressive environments, such as freeze/thaw (F/T) and wet/dry (W/D) cycling, especially along with attacks from the deicers. Although previous studies have pointed out that the failure of concrete products with exposure to an aggressive environment can be attributed to physical scaling and chemical reactions between the aggressive agents and the C-S-H binder phase, which synergistically result in the deterioration of the concrete products (Farnam et al., 2015; Qiao et al., 2018a), the

agreement of the chemical deteriorate mechanisms and the microstructure evolution process was yet achieved.

Numerous studies have reported that the deleterious process of concrete products is complicated and the damage mechanism is synergistic (Peterson et al., 2013; Xie et al., 2019). In a laboratory study, the deleterious process of concrete products with exposure to inorganic chemical solutions along with freeze/thaw and wet/dry cycles had been investigated. It was reported that all concrete products exhibited various mass and strength variations, and the microstructure of the cement hydration products was distinctively changed after a long term of soaking in the chemical solutions (Shi et al., 2013). In addition to the inorganic chemical solutions, the impact of the organic chemical solutions on the durability of concrete products has been studied (Xie et al., 2017). It was pointed out that the organic chemicals posed a negative impact on the durability of concrete products, especially for the concrete products prepared with reactive aggregates, which lead to the aggregate silicate reaction. The microstructure analysis demonstrated that the distress of the concrete was attributed to the leaching of the Ca from the C-S-H binder phase. Although the mechanical properties and durability of concrete products can be enhanced by many approaches such as using supplementary cementitious materials, fiber reinforcement, or water/binder ratio reduction, the side effects of these methods are also apparent, including high internal stress, thermal cracks, adhesion and corrosion problems of reinforced fibers. As a result, it is compelling to explore appropriate materials or technologies to mitigate the side effects of traditional modification methods.

In the past decades, it has been widely accepted that the hydration products of cementitious materials are composed of nanoscale phases (Xu and Viehland, 1996; Allen et al., 2007a; Allen and Thomas, 2007b). As a result, many studies have tried using nanomaterials to manipulate the microstructures of these nano-sized phases to enhance the durability of concrete products (Monteiro et al., 2009; Morsy et al., 2012; Lim and Mondal, 2014; Lu et al., 2015). The most widely used nanomaterials were titanium dioxide ( $\text{TiO}_2$ ) (Feng et al., 2013; Zhang et al., 2015), silica ( $\text{SiO}_2$ ) (Hou et al., 2013; Shiho et al., 2013; Singh et al., 2013), alumina ( $\text{Al}_2\text{O}_3$ ) (Nazari et al., 2010), iron oxide ( $\text{Fe}_2\text{O}_3$ ) (Li et al., 2004; Heikal, 2016), nano clay (Hakamy and Shaikh, 2014; Fan et al., 2015), and carbon nanomaterials (Morsy et al., 2011; Lv et al., 2013; Pan et al., 2015; Erdem et al., 2017; Luo et al., 2017; Zhou and Xie, 2020). It was claimed that with the addition of  $\text{TiO}_2$ ,  $\text{SiO}_2$ , and  $\text{Fe}_2\text{O}_3$  nanoparticles, the mechanical properties and wear resistance of the concrete products have been enhanced, and nano  $\text{TiO}_2$  had a higher modification effect than the nano  $\text{SiO}_2$  (Li et al., 2004; Li et al., 2006). Apart from nano  $\text{TiO}_2$  particles, the effects of nano  $\text{Al}_2\text{O}_3$  particles on the mechanical properties have been investigated. It was found that the 7 days compressive strength of concrete samples has enhanced by 30% and the 28 days elastic modulus has increased 143% with the addition of 5 wt%  $\text{Al}_2\text{O}_3$  nanoparticles (Li et al., 2006).

In addition to the mechanical properties, the environmental resistance of concrete products can also be considerably enhanced with the addition of nanoparticles (Lu, 2013; Shah, 2013).

Behfarnia investigated the freeze/thaw resistance of the concrete materials modified by nano-silica and nano alumina. The results indicated that, after 300 freeze/thaw cycles in water, the strength of the concrete samples with or without nano modification decreased 16 and 100%, respectively, (Behfarnia and Salemi, 2013). A similar statement was claimed that the addition of nano  $\text{SiO}_2$  and nano  $\text{Al}_2\text{O}_3$  has positive effects on the freeze/thaw resistance of concrete. With the addition of 5 wt% nano  $\text{SiO}_2$  or nano  $\text{Al}_2\text{O}_3$ , the freeze/thaw resistance of the concrete samples enhanced by over 80% comparing with the control samples (Salemi and Behfarnia, 2013).

Previous studies have stated that the modification mechanisms of the nanomaterials on the concrete materials can be attributed to the following reasons: 1) act as nano-sized fillers to decrease the nano-sized pores in the hydration products of the cementitious materials; 2) serve as the "nucleus" to align the hydration process and tune the microstructure evolution of the cementitious hydration products; 3) promote the forming of high-density C-S-H phase. Despite these mechanisms have been stated for many years, the modification mechanism of diverse nanomaterials on the properties of concrete materials remains unclear.

To elucidate the modification mechanism of the nanoparticles on the cement concrete, microstructure analysis is a promising method that can tell the impacts of nanoparticles on the microstructure evolution process. Scanning electron microscopy has been widely used to characterize the microstructure of concrete or cementitious materials with or without nano modification (Qing et al., 2007; Kong et al., 2012; Meng et al., 2012; Kong et al., 2013). According to the fracture surface morphology analysis, it can be found that the microstructures of Portland cement paste modified with nanomaterials are composed of  $\text{Ca}(\text{OH})_2$ , amorphous C-S-H phase, and pores (Li et al., 2004). Previous studies have assumed that the nanoparticles will act as nuclei to help growing new types of nanostructural hydration products, such as needle-shaped (or wire-shaped) hydration products. The EDS results showed that the needle-shaped hydration products were composed of Al, Ca, and Si with a Ca/Si ratio of 5:1 and Al/Si ratio of 3:5. Meanwhile, the adjacent area featured the Ca/Si and Al/Si ratio of 2:1 and 1:6, respectively, (Feng, 2012). Another study has also observed these needle-shaped hydration products and claimed them as ettringite. Based on the EDS analysis of the needle-shaped phases, it can be found that the main chemical composition of these phases was Ca, Al, and O, and a large amount of Si, little S was detected. Therefore, it can be deduced that the needle-shaped phase is more complicated than the ettringite.

Although the benefits of the nano modification are observable, the potential strengthening mechanisms are yet crystal clear. A few studies have argued that the benefits of the nano modification are questionable from the perspective of the nanoparticle types, especially with the addition of  $\text{Al}_2\text{O}_3$  nanoparticles. It was claimed that the nano  $\text{Al}_2\text{O}_3$  has negative effects on the durability enhancement of concrete products (León et al., 2014). Furthermore, to the best of our knowledge, limited studies were implemented to investigate the damage mechanism of nano-modified concrete with exposure to freeze/thaw cycling along with the attacks of  $\text{CaCl}_2$ . As a

**TABLE 1** | Mix design of the nano-modified concrete.

Water to cement ratio	Cement (kg/m <sup>3</sup> )	Water (kg/m <sup>3</sup> )	Fine aggregate (kg/m <sup>3</sup> )	Coarse aggregate (kg/m <sup>3</sup> )	Water reducer (%)
0.50	376	188	679	1,157	0.5

result, it is critical to find out the potential modification mechanism of diverse nanomaterials on the concrete products with exposure to the freeze/thaw and wet/dry cycles along with CaCl<sub>2</sub> attacks.

## EXPERIMENTAL METHODS AND MATERIALS

Ordinary Portland cement (P.O 42.5), natural sand, and basalt rocks were used as raw materials. Commercially available SiO<sub>2</sub> and Al<sub>2</sub>O<sub>3</sub> nanoparticles (provided by Hefei Liangziyuan Co.) were used as the modifiers. The purity of the nanomaterials was higher than 99.0%, and the average size and the specific surface area were about 30 nm and 80 m<sup>2</sup>/g, respectively.

The dosages of the nano modifiers were 0, 0.05, 0.1, 0.5, and 1.0% by the weight of cement. The water/cement ratio (w/c) was 0.5, and the mix proportion of the nano-modified concrete is listed in **Table 1**. To realize a dispersion condition of the nanoparticles, the naphthalene water reducer (UNF-5), with a content of 0.5 wt% of cement, was mixed in water via magnetic stirring with a mixing speed of 1,500 rpm for 5 min. Subsequently, the nano modifiers were added to the mixture and followed by sonication (200 w and 40 Hz) for 10 min. After sufficient mixing of the raw materials, the fresh concrete mixture was cast into steel molds with a size of 100 mm<sup>3</sup> × 100 mm<sup>3</sup> × 400 mm<sup>3</sup>. The specimens were de-molded after 24 h and cured in a moist room with relative humidity (RH) of 95% at 25°C for another 27 days. Once fully cured, the concrete specimens were air-dried for 24 h at 25°C at RH 45–55% and weighed before testing. The slump testing was based on the ASTM C143.

The impacts of the chemical attacks on the durability of nano-modified concrete products were evaluated by comparing the performance of concrete samples before and after freeze/thaw and wet/dry cycles in a diluted CaCl<sub>2</sub> solution with a concentration of 3 wt%. An accelerated manner of 3, 7, and 15 freeze/thaw and wet/dry cycles were used as the testing process. In each cycle, freezing the concrete samples in the diluted CaCl<sub>2</sub> solution at –25°C for 48 h and followed by thawing for 24 h and air-dried for another 12 h at room temperature (25°C, RH 50 ± 5%). The freezing and thawing rates were approximately 0.05 and 0.01°C/minute, respectively. After freeze/thaw and wet/dry cycles, the samples were washed and the scaled-off materials on the surface were removed by hands. Finally, the weights of the samples were recorded and the properties were tested accordingly. The compressive and flexural strengths of the concrete samples were determined using ASTM C39 and ASTM C496, respectively. The relative dynamic modulus of elasticity was obtained by testing the time of the supersonic wave passing through the concrete samples before and after

freeze/thaw and wet/dry cycles. The testing period was 0.4 μs with a voltage of 500 V. The relative dynamic modulus of elasticity was calculated based on the following equation:

$$R_n = \frac{t_0^2}{t_n^2} \times 100 \quad (1)$$

where  $R_n$  is the relative dynamic modulus of the concrete after  $n$  times of freeze/thaw and wet/dry cycles,  $t_0$  is the time that the supersonic wave passing through the concrete samples before freeze/thaw and wet/dry, and  $t_n$  is the time that the supersonic wave passing through the concrete samples after  $n$  times of freeze/thaw and wet/dry cycles.

The electric flux was tested according to GB/T 50082–2009. In this process, 28 days samples with a size of 150 mm × 150 mm × 150 mm × 51 mm. After properly connected, a constant 60 V direct current power was applied to the testing device, and the current values were recorded every 15 min. The final results were the average value of three samples.

The non-evaporable water content was obtained by calculating the mass change of the hardened paste before and after the calcination process. First, the samples were heated in air for 1 h at 85°C and then ground into powders. After an 80 μm sieving, the fine powders were dried at 105°C to reach a constant mass value and followed by calcination at 950°C for 1 h. The non-evaporable water can be calculated according to the following equation:

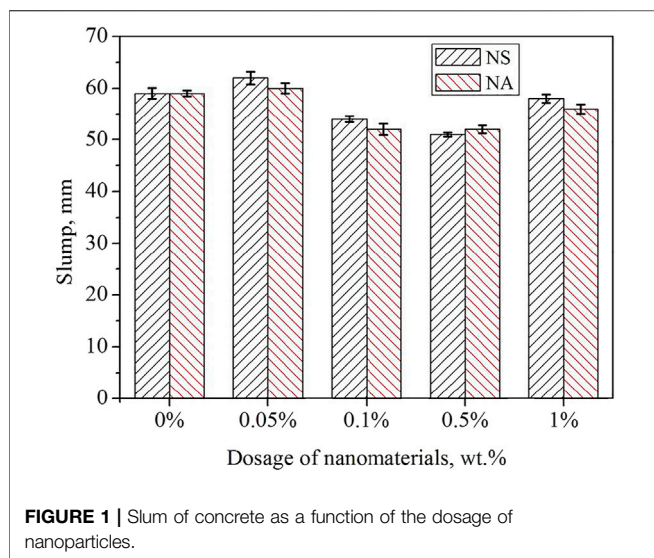
$$w_c = \frac{m_1 - m_2}{m_2} \times (100 - w_{LOI}) / w_{LOI} \quad (2)$$

where  $w_c$  is the content of the non-evaporable water,  $m_1$  and  $m_2$  are the mass of the cement powder before and after calcination, and  $w_{LOI}$  is the loss of ignition of the cement.

The heat of hydration was measured by TAM Air isothermal calorimeter with the inner mixing mode at 25°C. The temperature range of the thermogravimetric analysis (TA-SDT-Q600) was 30–800°C. A scanning electron microscope (FEI-Quanta 200F) coupled with energy-dispersive X-ray spectroscopy (EDS) analyzer was used to analyze the fracture surface morphologies of concrete samples before and after the freeze/thaw and wet/dry cycles in the CaCl<sub>2</sub> solution. The EDS results were obtained from the selected zone corresponding to the SEM morphology images. A typical 15–20 kV accelerating voltage was used with a scan time over 60 s per sampling area.

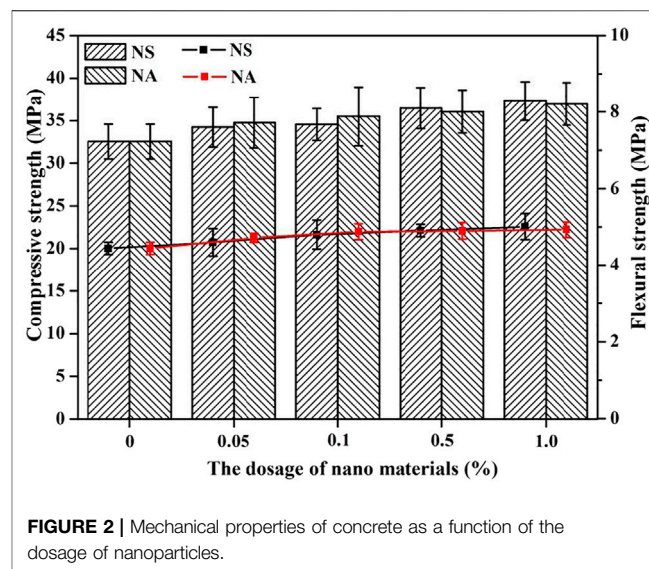
## RESULTS AND DISCUSSION

**Figure 1** gives the slump of fresh concrete samples as a function of the content of Al<sub>2</sub>O<sub>3</sub> nanoparticles via using nano SiO<sub>2</sub> as reference. As can be seen from this figure, the slump of the nano-



modified concrete was not distinctively reduced with increasing the dosage of nanoparticles when the dosage was lower than 1 wt %. The slumps of the nano SiO<sub>2</sub> and nano Al<sub>2</sub>O<sub>3</sub> modified concrete is lower than 65 mm, which is acceptable for field applications. Comparing with previous studies, the appropriate workability was originated from the low dosage of the nanomaterials. As demonstrated from this figure, the dosage of the nanomaterials was in a range of 0.05 to 1 wt%, which is lower than previous studies. If the contents of the nanomaterials increased from 1 to 5%, the workability of the concrete will be significantly decreased. It has been demonstrated that the high dosage addition of nanomaterials will significantly decrease the workability of the concrete (Nazari et al., 2010; Li et al., 2006). A few studies have even claimed that, if using the workability as the control parameter, the modification effect of nano Al<sub>2</sub>O<sub>3</sub> was not distinctive (Berra et al., 2012). Therefore, it is a critical issue to realize the mechanical properties enhancement without sacrifice the workability of nano-modified concrete. Comparing with increasing the water/binder ratio or the dosage of water reducers, decreasing the content of nanoparticles is a cost-effective method to prepare high property nano-modified concrete.

**Figure 2** shows the mechanical properties of concrete samples as a function of the dosage of nano SiO<sub>2</sub> and nano Al<sub>2</sub>O<sub>3</sub> particles. As demonstrated in this figure, the mechanical properties, including the compressive strength and the flexural strength, have been slightly increased with the increasing content of nanoparticles. Although the enhancement effect is not that distinctive, the average compressive strength of the nano-modified samples increased about 15% comparing with the control samples from 32.5 to 37.3 MPa and 37.0 MPa, respectively, with 1.0 wt% addition of nano SiO<sub>2</sub> and nano Al<sub>2</sub>O<sub>3</sub>. Similarly, the flexural strengths have also been slightly enhanced with the increasing content of the nanomaterials. Without the addition of nanomaterials, the flexural strength of the control sample was about 4.4 MPa, while with the addition of 1.0 wt% nano SiO<sub>2</sub> and nano Al<sub>2</sub>O<sub>3</sub> particles, the flexural

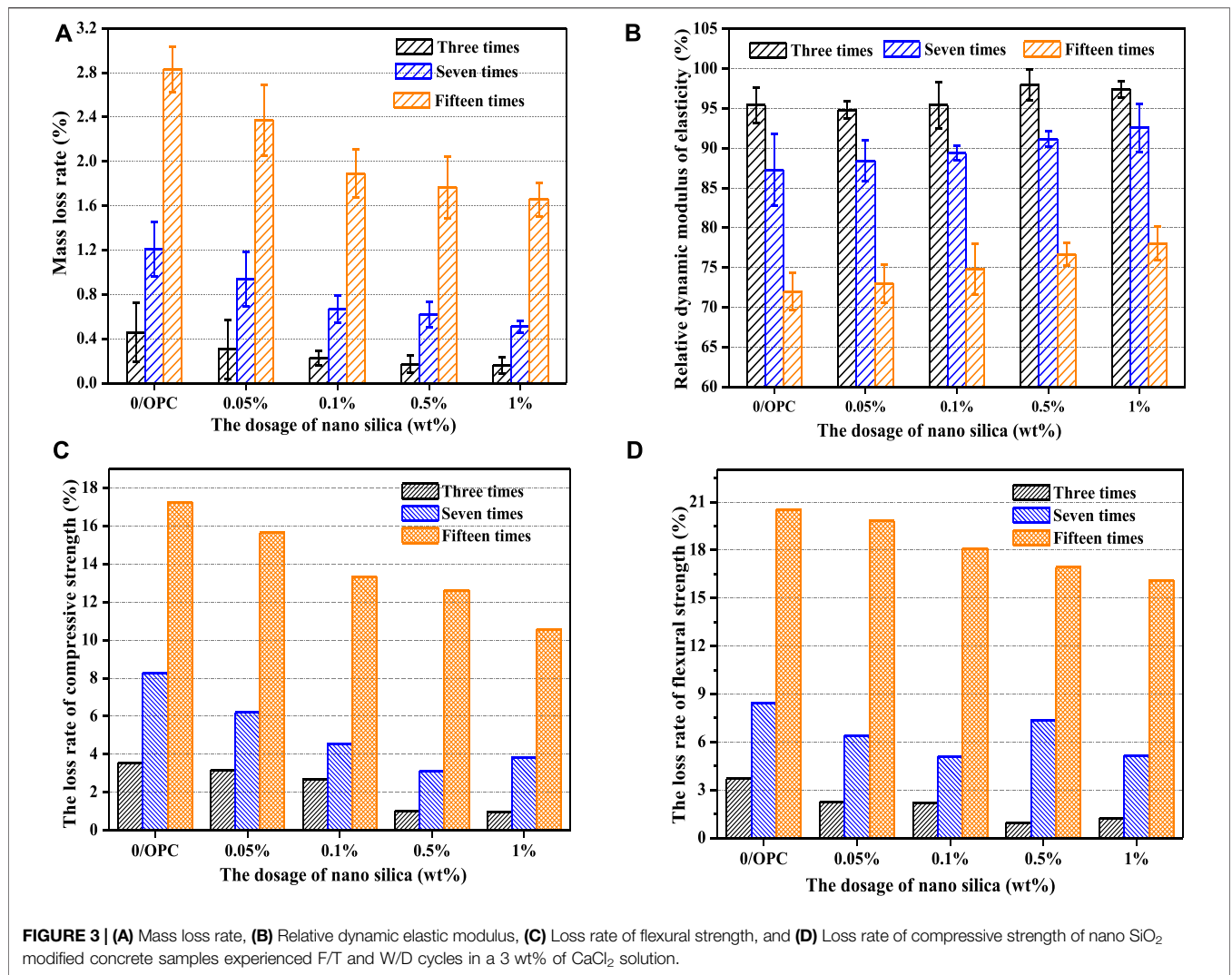


strengths have increased 11 and 13%, and reached 5.0 and 4.9 MPa, respectively.

The chemical resistance of the nano SiO<sub>2</sub> modified concrete samples with exposure to F/T and W/D cycles in a 3 wt% CaCl<sub>2</sub> solution is shown in **Figure 3**. As can be seen from **Figure 3A**), the mass loss of the concrete samples has considerably reduced with increasing contents of nano SiO<sub>2</sub>. Without the addition of nano SiO<sub>2</sub>, the mass loss was about 0.5, 1.2, and 2.8%, while with the addition of 1 wt% nano SiO<sub>2</sub>, the mass loss decreased to 0.2, 0.5, and 1.7%, after 3, 7, and 15 times of F/T and W/D cycles. Meanwhile, as demonstrated from **Figures 3B–D**), the nano modification effects on the relative dynamic modulus, the loss of compressive strength, and the loss of flexural strength are all observable. When the dosage of the nano SiO<sub>2</sub> increased from 0 to 1 wt%, the relative dynamic modulus increased from 95.4 to 97.4, 87.3–92.6, and 72.0–78.1% corresponding to 3, 7, and 15 times of F/T and W/D cycles. The loss of the compressive strength decreased from 3.5 to 0.9, 8.3–3.8, and 17.2–10.6% after 3, 7, and 15 F/T and W/D cycles. The loss of the flexural strength decreased from 3.7 to 1.2, 8.4–5.2, and 20.5–16.1% after 3, 7, and 15 F/T and W/D cycles.

Similar to the nano SiO<sub>2</sub>, nano Al<sub>2</sub>O<sub>3</sub> has been used as a modifier to strengthen the concrete products. It was claimed that the addition of nano Al<sub>2</sub>O<sub>3</sub> is beneficial to the mechanical properties of concrete products; however, the impact of nano Al<sub>2</sub>O<sub>3</sub> on the chemical resistance remains unclear. **Figure 4** shows the chemical resistance performance of concrete samples as a function of nano Al<sub>2</sub>O<sub>3</sub> contents. It can be found from the testing results, the mass loss of the nano Al<sub>2</sub>O<sub>3</sub> modified concrete decreased to 0.2, 0.6, and 1.8%, after 3, 7, and 15 times of F/T and W/D cycles in a 3 wt% CaCl<sub>2</sub> solution. With the contents of the nano Al<sub>2</sub>O<sub>3</sub> increased from 0 to 1 wt%, the relative dynamic modulus enhanced from 95.4 to 98.1%, 87.3–90.8%, and 72.0–76.6% corresponding to 3, 7, and 15 times of F/T and W/D cycles. The loss of the compressive strength decreased from 4.0 to 1.9, 7.9–6.0, and 17.5–14.5% after 3, 7, and 15 F/T and W/D cycles. The loss of the flexural strength decreased from





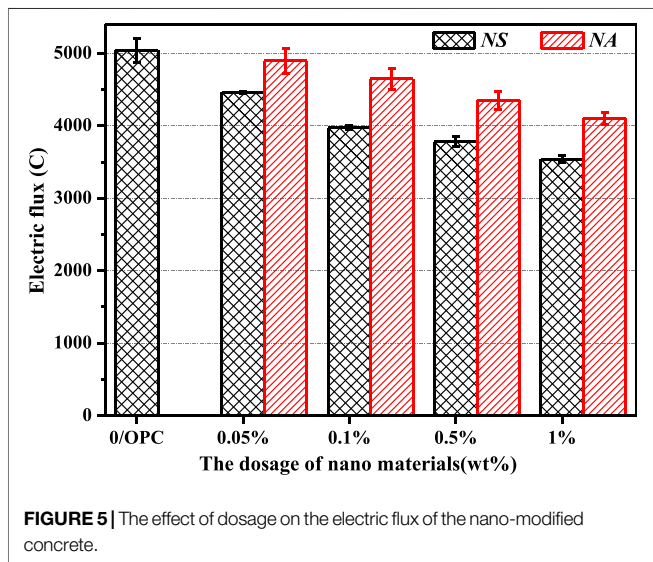
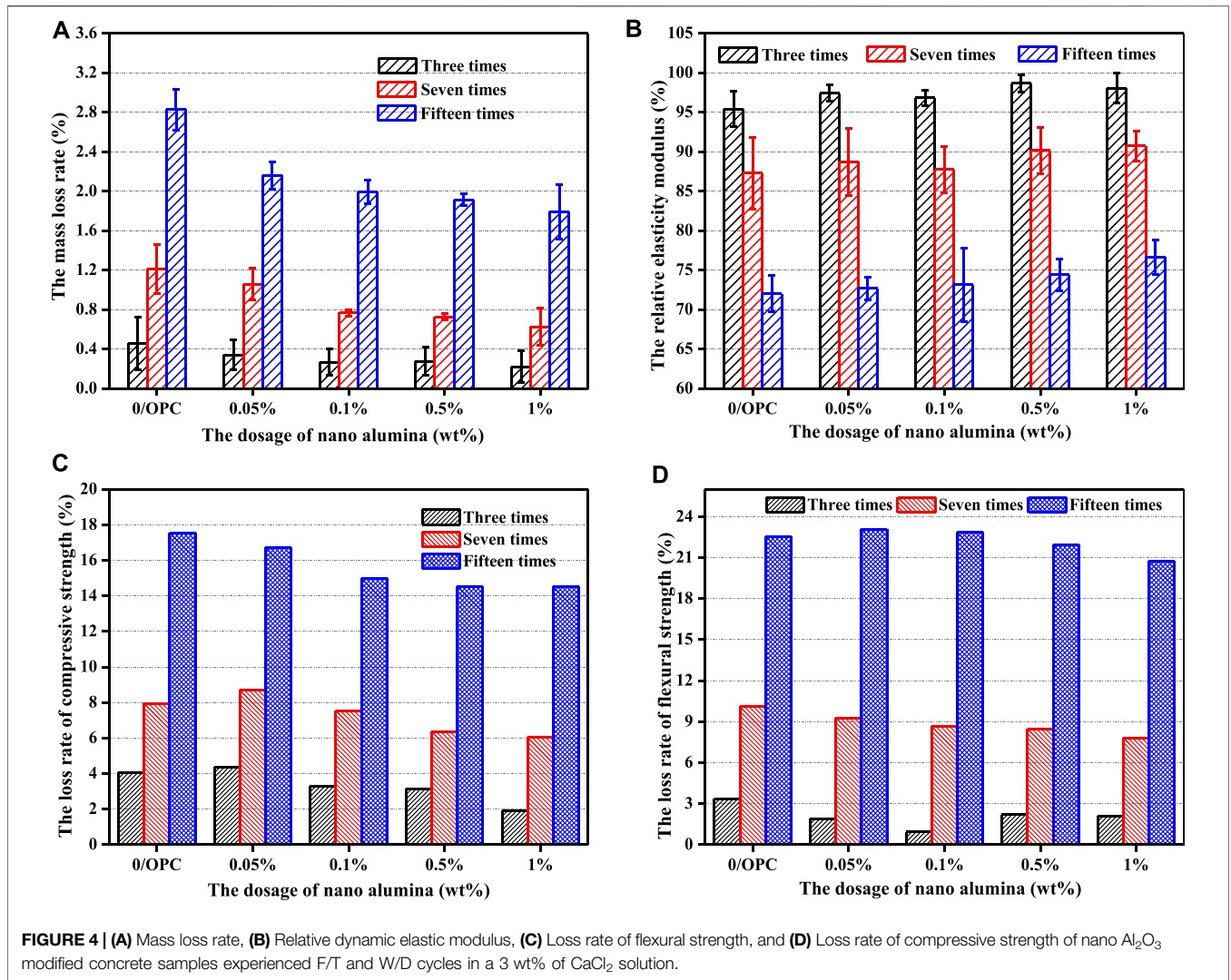
3.4 to 2.1, 10.1–7.8, and 22.6–20.7% after 3, 7, and 15 F/T and W/D cycles.

Figure 5 shows the electric flux of concrete samples as a function of the contents of nanoparticles. As can be seen from this figure, the electric flux of concrete samples decreased with increasing the contents of nanoparticles, especially when the dosage of nano SiO<sub>2</sub> reached 1.0 wt%, the electric flux of the samples was reduced by about 30%, from about 5,000 to 3,500 C. For the Al<sub>2</sub>O<sub>3</sub> nano-modified concrete samples, the electric flux reduced from 5,000 to about 4100 C when the dosage increased to 1.0 wt%, suggesting that the permeability of the concrete samples has been reduced by the addition of nano SiO<sub>2</sub> and nano Al<sub>2</sub>O<sub>3</sub>.

Figure 6 gives the isothermal calorimetry curves of the paste samples modified with nanoparticles. Figures 6A,B) demonstrate the total heat curves of the samples modified with nano SiO<sub>2</sub> and nano Al<sub>2</sub>O<sub>3</sub>, respectively. As can be seen from this figure, with the addition of nanoparticles, the hydration process has been distinctively changed. Although there is a slight fluctuation with the dosage of 0.5 wt%, the heat of hydration has considerably enhanced when the dosage of nanoparticles

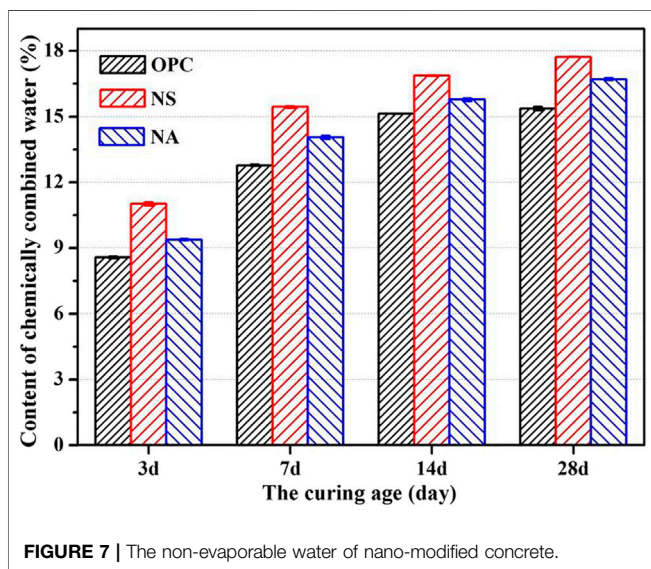
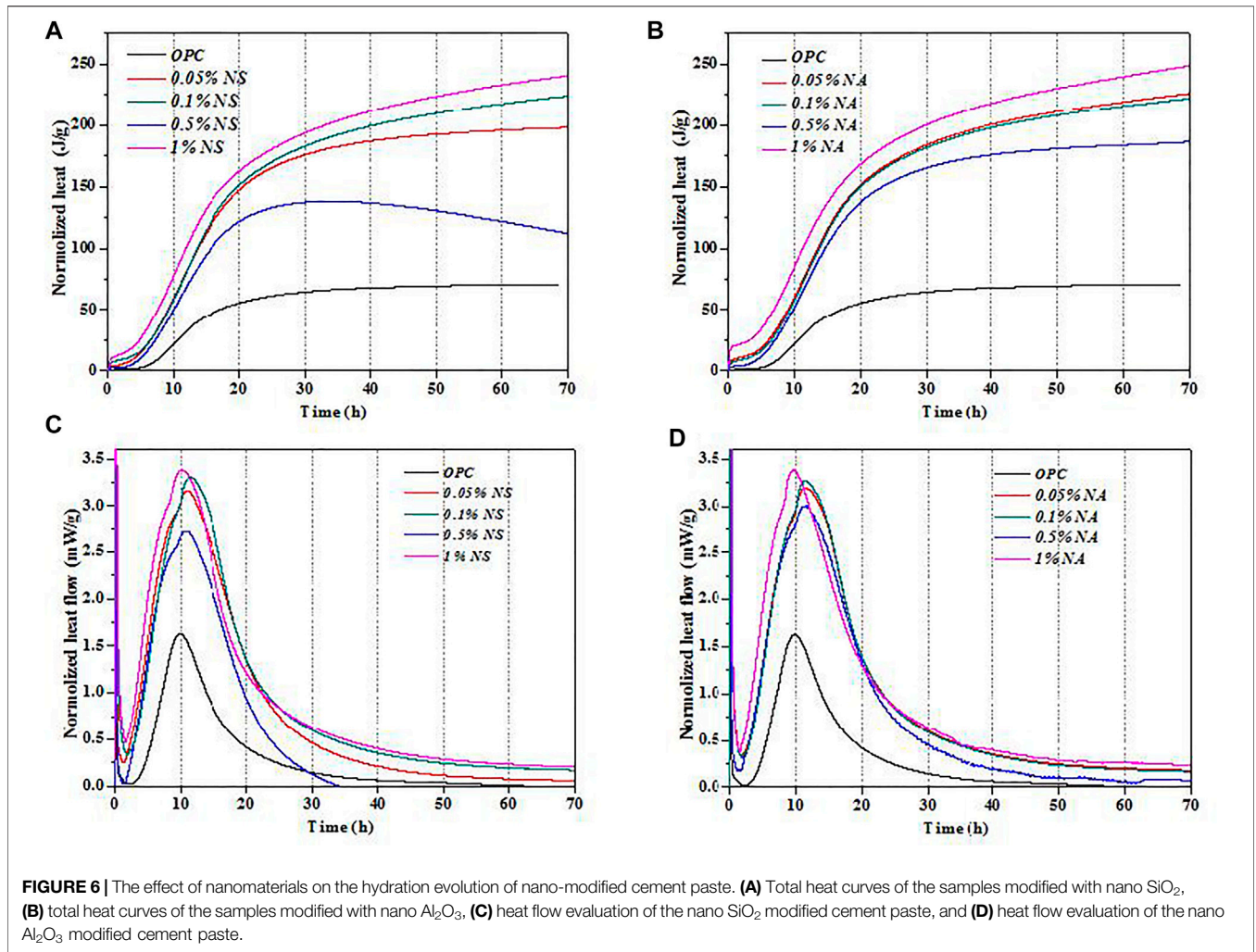
reached 1.0 wt%. Figures 6C,D) demonstrate the heat flow evaluation of the nano-modified cement paste samples corresponding to the same data group of Figures 6A,B). In Figures 6C,D), the hydration heat of C<sub>3</sub>A can be reflected by the first peak, and the hydration heat of C<sub>3</sub>S can be detected through the second peak. As demonstrated in this figure, the distinctive increase of the hydration heat indicates the addition of the nanoparticles is beneficial to the early age hydration process of cement paste.

The effect of nanoparticles on the non-evaporable water contents is shown in Figure 7. It can be observed that the content of the non-evaporable water has considerably increased with the addition of the nanoparticles. This phenomenon demonstrates that the content of chemically bonded water in the hydration products can be increased because of the addition of the nanoparticles. Besides, the nano SiO<sub>2</sub> shows a higher enhancement effect than the nano Al<sub>2</sub>O<sub>3</sub>. This mainly results from the pozzolanic activity of nano SiO<sub>2</sub>, which is beneficial to form more C-S-H phases (xCaO•ySiO<sub>2</sub>•zH<sub>2</sub>O, C-S-H gel). Meanwhile, although the



effect of nano Al<sub>2</sub>O<sub>3</sub> is less than the nano SiO<sub>2</sub>, it still has a remarkable enhancement by comparing with the control samples. Previous studies have claimed that the amount of hydration products is proportional to the contents of the non-evaporable water. Therefore, it is reasonable to claim that nano SiO<sub>2</sub> and Al<sub>2</sub>O<sub>3</sub> are beneficial to optimize the phase structures.

Different from the physical F/T scaling process, the deterioration of concrete with exposure to F/T, W/D, and chemical attacks is attributed to both physical and chemical mechanisms. The physical F/T damage mainly resulted from the hydraulic pressure, which is determined by the permeability of concrete materials, while the chemical deterioration is governed by the chemical reaction between the aggressive agents and the cementitious binder phases (Xie et al., 2017; Xie et al., 2019; Qiao et al., 2018a; Qiao et al., 2018b). According to the results from previous studies, it has been widely accepted that the CaCl<sub>2</sub> will react with the Ca(OH)<sub>2</sub> and form the volume expansive calcium oxychloride (CaCl<sub>2</sub>·3Ca(OH)<sub>2</sub>·12H<sub>2</sub>O), which increase the internal stress

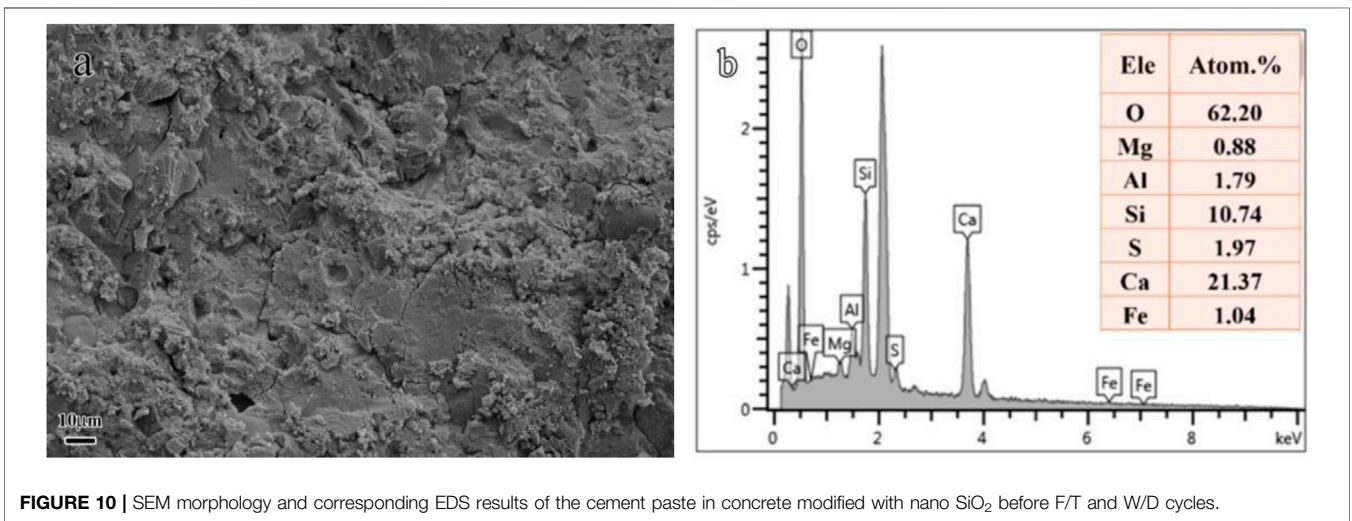
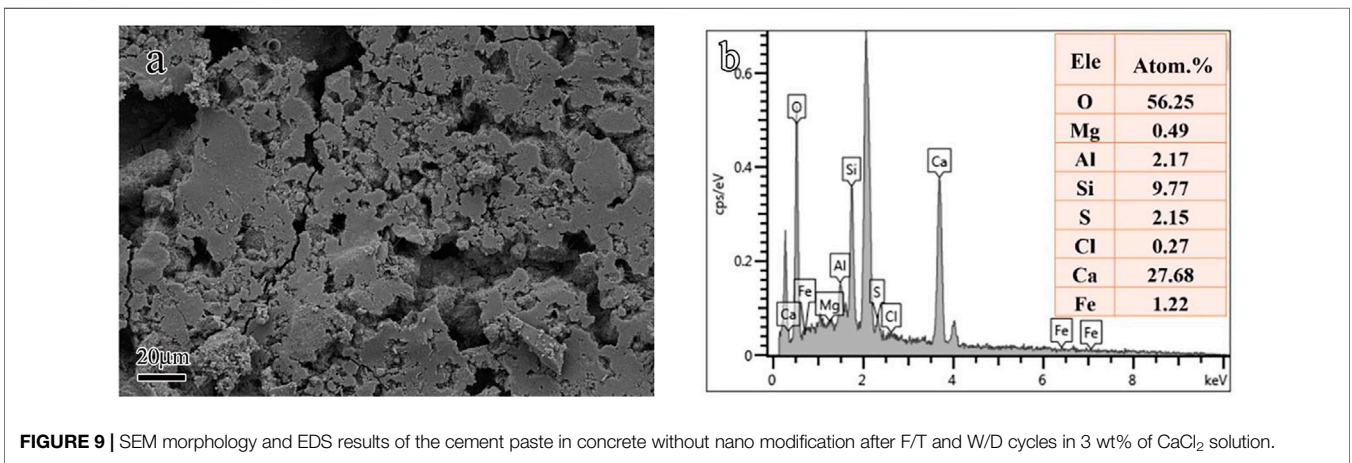
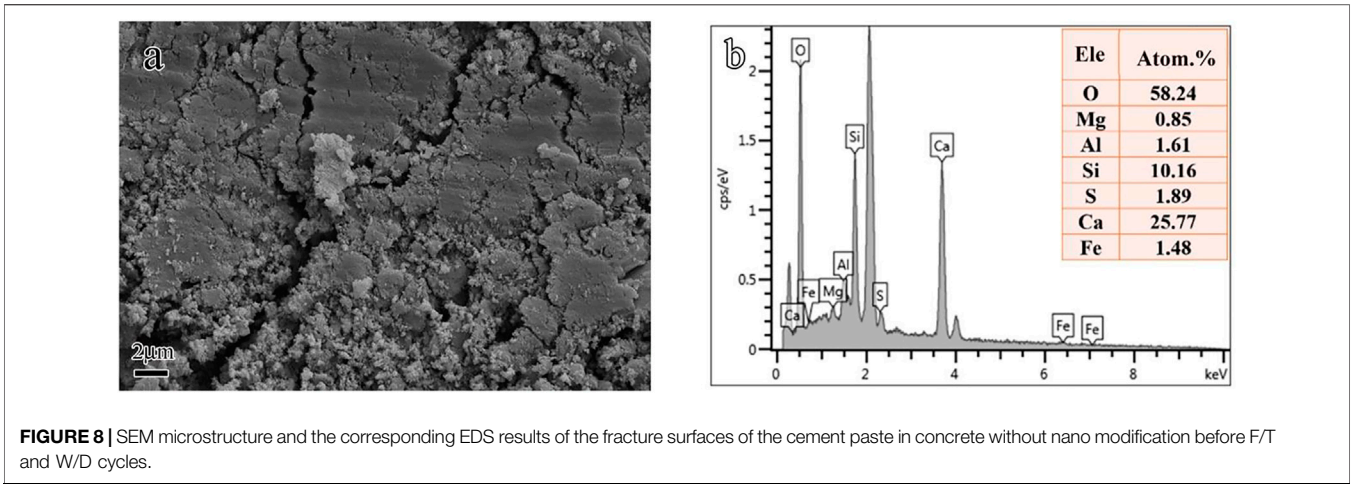


and results in the failure of concrete products (Farnam et al., 2015; Qiao et al., 2019).

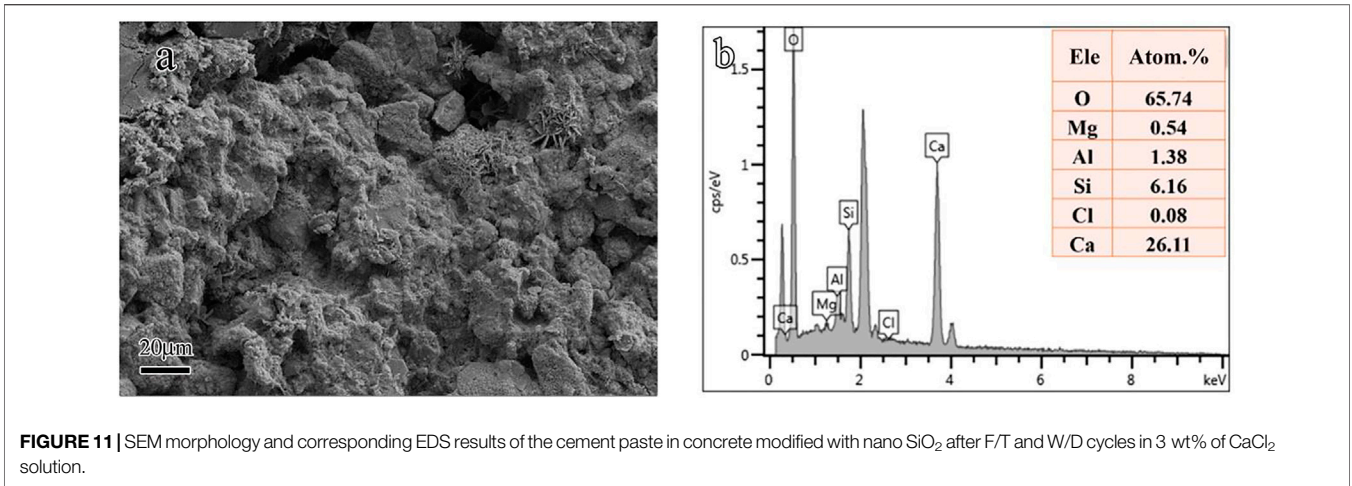
Figures 8, 9 depict the fracture surface SEM morphologies and the corresponding EDS analysis of the control cement paste samples before and after F/T along with W/D cycles in a 3 wt% of CaCl<sub>2</sub> solution. As can be seen from Figure 8, without the F/T and W/D cycles in the CaCl<sub>2</sub> solution, the microstructure of the control paste sample is quite dense. The EDS result shows that the Ca/Si ratio is about 2.5, and no Cl can be detected. While after the F/T and W/D cycles in CaCl<sub>2</sub> solution, the microstructure of the cement paste start to have continuous pores in the dense cementitious phase, and a colloidal precipitation layer was affiliated on the surface of the binder phase. The corresponding EDS results indicate that the Ca and Cl contents are slightly higher than the control sample, while the Si and Fe contents remain similar values.

Figures 10, 11 illustrate the SEM fracture surface microstructure and the corresponding EDS results of the



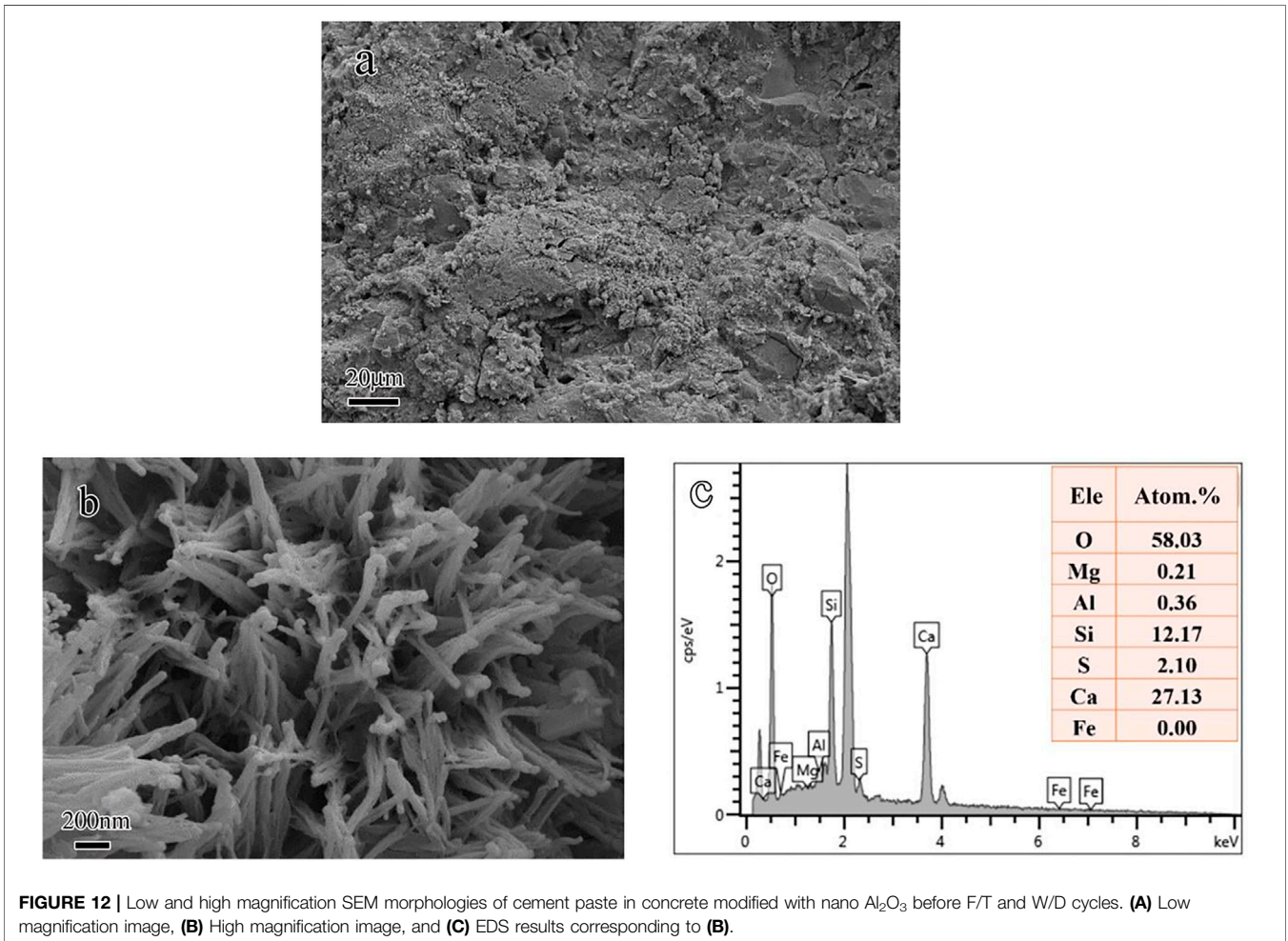






cement paste samples modified with nano SiO<sub>2</sub> before and after F/T along with W/D cycles in a 3 wt% of CaCl<sub>2</sub> solution. As shown in **Figure 10**, before the F/T and W/D cycles in CaCl<sub>2</sub> solution, coral shape hydration products can be observed, and the microstructure of the sample is quite

dense. This is well agreed with the results from previous studies that the addition of nano SiO<sub>2</sub> is beneficial to form high-density hydration products (Shah, 2013; Hou et al., 2013). The EDS result shows that the Ca/Si ratio is about 2.0, and a small amount of S can be detected. Similar to the



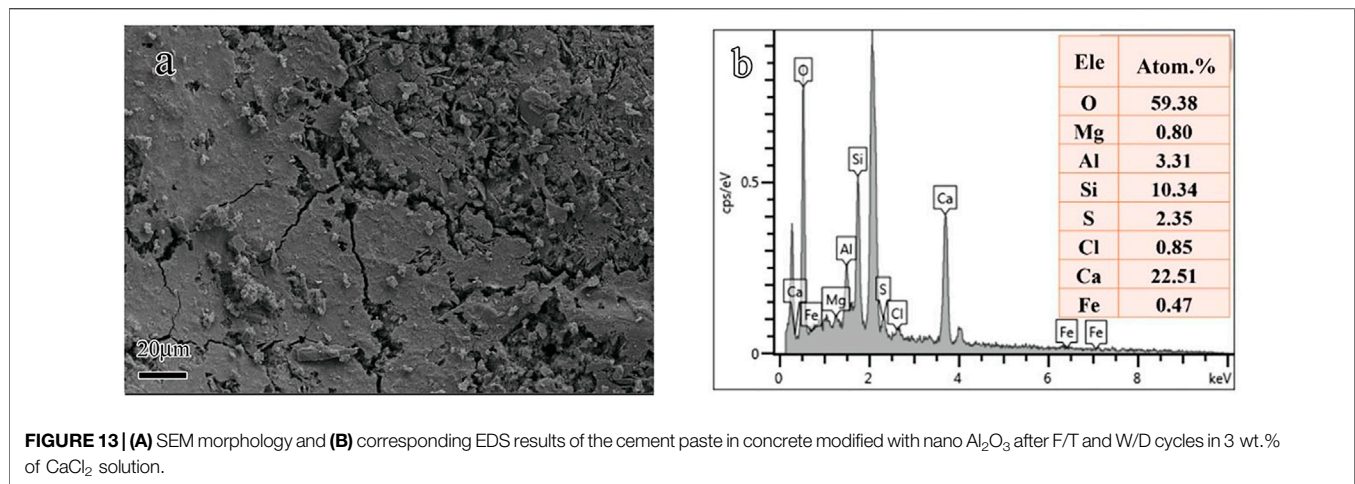


**FIGURE 13 | (A)** SEM morphology and **(B)** corresponding EDS results of the cement paste in concrete modified with nano  $\text{Al}_2\text{O}_3$  after F/T and W/D cycles in 3 wt.% of  $\text{CaCl}_2$  solution.

microstructure of cement paste without nano modification, after the F/T and W/D cycles in  $\text{CaCl}_2$  solution, the dense structure of the binder phase has been broken, and a colloidal precipitation layer was affiliated on the surface of the binder phase. The corresponding EDS results indicate that the Ca/Si ratio has changed to about 4.3, and the Cl can be detected.

**Figures 12, 13** demonstrate the microstructure and the corresponding EDS results of the nano  $\text{Al}_2\text{O}_3$  modified cement paste before and after F/T along with W/D cycles in a 3 wt% of  $\text{CaCl}_2$  solution. As can be seen from the low magnification fracture surface morphology (**Figure 12A**), without the F/T and W/D cycles in  $\text{CaCl}_2$  solution, the microstructure of the nano  $\text{Al}_2\text{O}_3$  modified sample is also quite dense and no distinctive cracks or pores can be detected. Furthermore, it can be observed from the high magnification microstructure (**Figure 12B**), needle shape hydration products can be observed. The corresponding EDS result of this needle shape hydration product demonstrates that the Ca/Si ratio of this phase is about 2.3, a small amount of S, and no Cl can be detected. While after the F/T and W/D cycles in the  $\text{CaCl}_2$  solution, similar to previous ones, a large number of colloidal precipitates can be observed on the surface of the binder phase. The corresponding EDS results indicate that the Ca/Si ratio has become 2.0, and the Al content is relatively higher than the other samples.

## CONCLUSION

This work presents a comparative result to investigate the impacts of  $\text{CaCl}_2$  along with F/T and W/D cycles on the durability of concrete products modified with nano  $\text{SiO}_2$  and nano  $\text{Al}_2\text{O}_3$ . It was found that the environmental resistance of concrete materials can be remarkably enhanced with the addition of nanoparticles. The compressive and flexural strengths have increased about 15 and 13%, respectively, corresponding to the dosage of 1.0 wt% of nano  $\text{SiO}_2$  and nano  $\text{Al}_2\text{O}_3$ . The electric flux has significantly decreased from 5,000 to 3,500°C and 4,100, suggesting the

reduction of the permeability. Besides, the heat of hydration testing results demonstrates that the nano  $\text{SiO}_2$  and nano  $\text{Al}_2\text{O}_3$  have considerable impacts on accelerating the hydration process. The non-evaporable water contents have reduced with increasing contents of nano  $\text{SiO}_2$  and nano  $\text{Al}_2\text{O}_3$ . The SEM/EDS analysis demonstrates that the high-density C-S-H phase will be formed. After the F/T and W/D cycles in a  $\text{CaCl}_2$  solution, although colloidal precipitates will be formed and the dense microstructure of the cement paste will be damaged, the addition of nanoparticles is beneficial to remain the dense structure of cement paste.

## DATA AVAILABILITY STATEMENT

The original contributions presented in the study are included in the article/Supplementary Material, further inquiries can be directed to the corresponding authors.

## AUTHOR CONTRIBUTIONS

YZ wrote most of this manuscript. YZ was in charge of implementing most of the materials manufacturing and properties testing. NX helped on the microstructure analysis, PH and LF helped the discussion and analyzing parts. NC and SZ organized the outline and the whole contents. All authors have read and agreed to the published version of the manuscript.

## FUNDING

This research was funded by the National Key R&D Program of China (2017YFB0310003), National Natural Science Foundation of China (Project Nos. 51772128 and 51632003), Youth Innovation Support Program of Shandong Colleges and Universities, Taishan Scholar Program, Case-by-Case Project for Top Outstanding Talents of Jinan, Double Hundred Foreign Expert Program (WST2018011), and Lianyungang

Gaoxin District International Scientific Cooperation Program (HZ201902), Sino-European Research Center program (SERC-M-20191201), and Lianyungang Haiyan Plan program (2019-

QD-002). Some or all data, models, or code that support the findings of this study are available from the corresponding author upon reasonable request.

## REFERENCES

- Allen, A. J., and Thomas, J. J. (2007b). Analysis of C-S-H Gel and Cement Paste by Small-Angle Neutron Scattering. *Cement Concrete Res.* 37, 319–324. doi:10.1016/j.cemconres.2006.09.002
- Allen, A. J., Thomas, J. J., and Jennings, H. M. (2007a). Composition and Density of Nanoscale Calcium-Silicate-Hydrate in Cement. *Nat. Mater* 6, 311–316. doi:10.1038/nmat1871
- Behfarnia, K., and Salemi, N. (2013). The Effects of Nano-Silica and Nano-Alumina on Frost Resistance of normal concrete. *Construction Building Mater.* 48, 580–584. doi:10.1016/j.conbuildmat.2013.07.088
- Berra, M., Carassiti, F., Mangialardi, T., Paolini, A. E., and Sebastiani, M. (2012). Effects of Nanosilica Addition on Workability and Compressive Strength of Portland Cement Pastes. *Construction Building Mater.* 35, 666–675. doi:10.1016/j.conbuildmat.2012.04.132
- Erdem, S., Hanbay, S., and Blankson, M. A. (2017). Self-sensing Damage Assessment and Image-Based Surface Crack Quantification of Carbon Nanofibre Reinforced concrete. *Construction Building Mater.* 134, 520–529. doi:10.1016/j.conbuildmat.2016.12.197
- Fan, Y., Zhang, S., Wang, Q., and Shah, S. P. (2015). Effects of Nano-Kaolinite clay on the Freeze-Thaw Resistance of concrete. *Cement and Concrete Composites* 62, 1–12. doi:10.1016/j.cemconcomp.2015.05.001
- Farnam, Y., Wiese, A., Bentz, D., Davis, J., and Weiss, J. (2015). Damage Development in Cementitious Materials Exposed to Magnesium Chloride Deicing Salt. *Construction Building Mater.* 93, 384–392. doi:10.1016/j.conbuildmat.2015.06.004
- Feng, D., Xie, N., Gong, C., Leng, Z., Xiao, H., Li, H., et al. (2013). Portland Cement Paste Modified by TiO<sub>2</sub>Nanoparticles: A Microstructure Perspective. *Ind. Eng. Chem. Res.* 52 (33), 11575–11582. doi:10.1021/ie4011595
- Hakamy, A., Shaikh, F. U. A., and Low, I. M. (2014). Thermal and Mechanical Properties of Hemp Fabric-Reinforced Nanoclay-Cement nanocomposites Thermal and Mechanical Properties of Hemp Fabric-Reinforced Nanoclay-Cement Nanocomposites. *J. Mater. Sci.* 49 (4), 1684–1694. doi:10.1007/s10853-013-7853-0
- Heikal, M. (2016). Characteristics, Textural Properties and Fire Resistance of Cement Pastes Containing Fe<sub>2</sub>O<sub>3</sub> Nano-Particles. *J. Therm. Anal. Calorim.* 126 (3), 1077–1087. doi:10.1007/s10973-016-5715-0
- Hou, P., Kawashima, S., Kong, D., CorrCorr, D. J., Qian, J., and Shah, S. P. (2013). Modification Effects of Colloidal nanoSiO<sub>2</sub> on Cement Hydration and its Gel Property. *Composites B: Eng.* 45 (1), 440–448. doi:10.1016/j.compositesb.2012.05.056
- Kong, D., Du, X., Wei, S., Zhang, H., Yang, Y., and Shah, S. P. (2012). Influence of Nano-Silica Agglomeration on Microstructure and Properties of the Hardened Cement-Based Materials. *Construction Building Mater.* 37, 707–715. doi:10.1016/j.conbuildmat.2012.08.006
- Kong, D., Su, Y., Du, X., Yang, Y., Wei, S., and Shah, S. P. (2013). Influence of Nano-Silica Agglomeration on Fresh Properties of Cement Pastes. *Construction Building Mater.* 43, 557–562. doi:10.1016/j.conbuildmat.2013.02.066
- León, N., Massana, J., Alonso, F., Moragues, A., and Sánchez-Espinosa, E. (2014). Effect of Nano-SiO<sub>2</sub> and Nano-Al<sub>2</sub>O<sub>3</sub> on Cement Mortars for Use in Agriculture and Livestock Production. *Biosyst. Eng.* 123, 1–11. doi:10.1016/j.biosystemseng.2014.04.009
- Li, H., Xiao, H.-g., Yuan, J., and Ou, J. (2004). Microstructure of Cement Mortar with Nano-Particles. *Composites Part B: Eng.* 35 (2), 185–189. doi:10.1016/s1359-8368(03)00052-0
- Li, H., Zhang, M.-h., and Ou, J.-p. (2006). Abrasion Resistance of concrete Containing Nano-Particles for Pavement. *Wear* 260, 1262–1266. doi:10.1016/j.wear.2005.08.006
- Lim, S., and Mondal, P. (2014). Micro- and Nano-Scale Characterization to Study the thermal Degradation of Cement-Based Materials. *Mater. Characterization* 92, 15–25. doi:10.1016/j.matchar.2014.02.010
- Lu, S.-N., Xie, N., Feng, L.-C., and Zhong, J. (2015). Applications of Nanostructured Carbon Materials in Constructions: The State of the Art. *J. Nanomater.* 2015, 6.
- Luo, J., Hou, D., Li, Q., Wu, C., and Zhang, C. (2017). Comprehensive Performances of Carbon Nanotube Reinforced Foam concrete with Tetraethyl Orthosilicate Impregnation. *Construction Building Mater.* 131, 512–516. doi:10.1016/j.conbuildmat.2016.11.105
- Lv, S., Ma, Y., Qiu, C., Sun, T., Liu, J., and Zhou, Q. (2013). Effect of Graphene Oxide Nanosheets of Microstructure and Mechanical Properties of Cement Composites. *Construction Building Mater.* 49, 121–127. doi:10.1016/j.conbuildmat.2013.08.022
- Meng, T., Yu, Y., Qian, X., Zhan, S., and Qian, K. (2012). Effect of Nano-TiO<sub>2</sub> on the Mechanical Properties of Cement Mortar. *Construction Building Mater.* 29, 241–245. doi:10.1016/j.conbuildmat.2011.10.047
- Monteiro, P. J. M., Kirchheim, A. P., Chae, S., Fischer, P., MacDowell, A. A., Schaible, E., et al. (2009). Characterizing the Nano and Micro Structure of concrete to Improve its Durability. *Cement and Concrete Composites* 31, 577–584. doi:10.1016/j.cemconcomp.2008.12.007
- Morsy, M. S., Al-Salloum, Y. A., Abbas, H., and Alsayed, S. H. (2012). Behavior of Blended Cement Mortars Containing Nano-Metakaolin at Elevated Temperatures. *Construction Building Mater.* 35, 900–905. doi:10.1016/j.conbuildmat.2012.04.099
- Morsy, M. S., Alsayed, S. H., and Aqel, M. (2011). Hybrid Effect of Carbon Nanotube and Nano-clay on Physico-Mechanical Properties of Cement Mortar. *Construction Building Mater.* 25 (1), 145–149. doi:10.1016/j.conbuildmat.2010.06.046
- Nazari, A., Riahi, S., Riahi, S., Shamekhi, S. F., and Khademno, A. (2010). Influence of Al<sub>2</sub>O<sub>3</sub> Nanoparticles on the Compressive Strength and Workability of Blended concrete. *J. Am. Sci.* 6, 6–9.
- Pan, Z., He, L., Qiu, L., Korayem, A. H., Li, G., Zhu, J. W., et al. (2015). Mechanical Properties and Microstructure of a Graphene Oxide-Cement Composite. *Cement and Concrete Composites* 58, 140–147. doi:10.1016/j.cemconcomp.2015.02.001
- Peterson, K., Julio-Betancourt, G., Sutter, L., Hooton, R. D., and Johnston, D. (2013). Observations of Chloride Ingress and Calcium Oxychloride Formation in Laboratory concrete and Mortar at 5°C. *Cement Concrete Res.* 45, 79–90. doi:10.1016/j.cemconres.2013.01.001
- Qiao, C., Suraneni, P., Nathalene Wei Ying, T., Choudhary, A., and Weiss, J. (2019). Chloride Binding of Cement Pastes with Fly Ash Exposed to CaCl<sub>2</sub> Solutions at 5 and 23 °C. *Cement and Concrete Composites* 97, 43–53. doi:10.1016/j.cemconcomp.2018.12.011
- Qiao, C., Suraneni, P., and Weiss, J. (2018a). Flexural Strength Reduction of Cement Pastes Exposed to CaCl<sub>2</sub> Solutions. *Cement and Concrete Composites* 86, 297–305. doi:10.1016/j.cemconcomp.2017.11.021
- Qiao, C., Suraneni, P., and Weiss, J. (2018b). Flexural Strength Reduction of Cement Pastes Exposed to CaCl<sub>2</sub> Solutions. *Cement and Concrete Composites* 86, 297–305. doi:10.1016/j.cemconcomp.2017.11.021
- Qing, Y., Zenan, Z., Deyu, K., and Rongshen, C. (2007). Influence of Nano-SiO<sub>2</sub> Addition on Properties of Hardened Cement Paste as Compared with Silica Fume. *Construction Building Mater.* 21 (3), 539–545. doi:10.1016/j.conbuildmat.2005.09.001
- Salemi, N., and Behfarnia, K. (2013). Effect of Nano-Particles on Durability of Fiber-Reinforced concrete Pavement. *Construction Building Mater.* 48, 934–941. doi:10.1016/j.conbuildmat.2013.07.037
- Shi, X., Veneziano, D., Xie, N., and Gong, J. (2013). Use of Chloride-Based Ice Control Products for Sustainable winter Maintenance: A Balanced Perspective. *Cold Regions Sci. Technology* 86, 104–112. doi:10.1016/j.coldregions.2012.11.001
- Shiho, K., Hou, P., David, J., and Shah, S. P. (2013). Modification of Cement-Based Materials with Nanoparticles. *Cement and Concrete Composites* 36, 8–15. doi:10.1016/j.cemconcomp.2012.06.012
- Singh, L. P., Karade, S. R., Bhattacharyya, S. K., Yousuf, M. M., and Ahalawat, S. (2013). Beneficial Role of Nanosilica in Cement Based Materials - A Review. *Construction Building Mater.* 47, 1069–1077. doi:10.1016/j.conbuildmat.2013.05.052



- Xie, N., Dang, Y., and Shi, X. (2019). New Insights into How MgCl<sub>2</sub> Deteriorates Portland Cement concrete. *Cement Concrete Res.* 120, 244–255. doi:10.1016/j.cemconres.2019.03.026
- Xie, N., Shi, X., and Zhang, Y. (2017). Impacts of Potassium Acetate and Sodium-Chloride Deicers on concrete. *J. Mater. Civil Eng.* 29, 04016229. doi:10.1061/(asce)mt.1943-5533.0001754
- Xu, Z., and Viehland, D. (1996). Observation of a Mesostructure in Calcium Silicate Hydrate Gels of Portland Cement. *Phys. Rev. Lett.* 77, 952–955. doi:10.1103/physrevlett.77.952
- Zhang, R., Cheng, X., Hou, P., and Ye, Z. (2015). Influences of Nano-TiO<sub>2</sub> on the Properties of Cement-Based Materials: Hydration and Drying Shrinkage. *Construction Building Mater.* 81, 35–41. doi:10.1016/j.conbuildmat.2015.02.003
- Zhou, Z., Xie, N., Cheng, X., Feng, L., Hou, P., Huang, S., et al. (2020). Electrical Properties of Low Dosage Carbon Nanofiber/cement Composite: Percolation

Behavior and Polarization Effect. *Cement and Concrete Composites* 109, 103539. doi:10.1016/j.cemconcomp.2020.103539

**Conflict of Interest:** The authors declare that the research was conducted in the absence of any commercial or financial relationships that could be construed as a potential conflict of interest.

Copyright © 2021 Zhao, Cui, Zhao, Zhu, Hou, Feng and Xie. This is an open-access article distributed under the terms of the Creative Commons Attribution License (CC BY). The use, distribution or reproduction in other forums is permitted, provided the original author(s) and the copyright owner(s) are credited and that the original publication in this journal is cited, in accordance with accepted academic practice. No use, distribution or reproduction is permitted which does not comply with these terms.